Theoret.Appl.Mech. TEOPM7, Vol.40,No.3,pp.441–464, Belgrade 2013*

ENTROPY ANALYSIS FOR THIRD-GRADE FLUID FLOW WITH TEMPERATURE-DEPENDENT VISCOSITY IN ANNULUS PARTIALLY FILLED WITH POROUS MEDIUM

Dileep Singh Chauhan **Vikas Kumar**

*doi:10.2298/TAM1303441C Math. Subj. Class.: 76A05; 76R50; 76S05.

According to: *Tib Journal Abbreviations (C) Mathematical Reviews*, the abbreviation TEOPM7 stands for TEORIJSKA I PRIMENJENA MEHANIKA.

Theoret. Appl. Mech., Vol.40, No.3, pp. 441–464, Belgrade 2013

Entropy analysis for third-grade fluid flow with temperature-dependent viscosity in annulus partially filled with porous medium

Dileep Singh Chauhan* **Vikas Kumar†**

Abstract

In the present paper, a non-Newtonian third-grade fluid flow is considered in an annulus partially filled by a porous medium of very small permeability. An analytical solution by the perturbation series method is obtained for velocity and temperature fields, assuming Reynolds's model to account for the variation of fluid viscosity with temperature. The effects of various pertinent parameters on the flow field, temperature field and entropy generation number are obtained and discussed graphically.

Keywords: Annulus, third-grade fluid, entropy generation number, permeability and porous medium

1 Introduction

A study on heat transfer in flow through pipes and annular pipes is important from both engineering and scientific points of view. Pipes and concentric annular pipes are often encountered in several engineering and industrial engineering applications such as oil well drilling, lubricants in journal bearing, cooling channels in gas turbine blades and nuclear reactors, physiology, various heat exchangers, and transpirations cooling.

Berman [1] obtained closed form solution for a Newtonian fluid flow through a porous annulus. The extensions of this flow problem to non-Newtonian fluids and heat transfer have been investigated, because of their applications in biophysical flows, artificial dialysis, oil field operations, food preservation, technology and industry, by several researchers such as Kapur and Goel [2], Mishra

*Department of Mathematics, University of Rajasthan, Jaipur-302004, India, e-mail: dileepschauhan@gmail.com

†Department of Mathematics, University of Rajasthan, Jaipur-302004, India

and Roy [3,4], Hecht [5], Sharma and Singh [6], and Bhatnagar *et al.* [7]. Wang and Chukwu [8] studied unsteady axial couette flow of non-Newtonian power-law fluids in concentric annulus. Yürüsoy and Pakdemirli [9] and Yürüsoy [10] examined flow of a third grade non-Newtonian fluid in a pipe and between concentric circular cylinders respectively. Erdogan and Imrak [11] investigated steady flow of a second-grade non-Newtonian fluid through an annulus with porous boundaries.

The axial flow of Newtonian and non-Newtonian fluids through an annulus or tube filled or partially filled with a porous medium and the associated heat transfer have many important applications in cooling and heating systems, ventilation and air-conditioning systems, nuclear reactors and heat exchangers. Chikh *et al.* [12] obtained an analytical solution of non-Darcian forced convection flow through an annular duct which is partially filled with a porous medium. Demirel and Kahraman [13] studied convective heat transfer effects in an annular packed bed. Scurtu *et al.* [14] investigated natural convection in the annulus between two concentric horizontal cylinders filled with a fluid-saturated porous medium. A theoretical analysis of heat transfer effects was investigated by Haji-Sheikh [15] and Minkowycz and Haji-Sheikh [16] in parallel plates and circular ducts filled with fluid saturated porous medium. Forced convection flow analysis was conducted by Hooman and Gurgenci [17], Hooman *et al.* [18, 19], Kuznetsov *et al.* [20] in a porous saturated circular tube. Numerical analysis was conducted by Khanafer *et al.* [21] of free convection in a horizontal annulus partially filled with a fluid-saturated porous medium. Al-Zahrani and Kiwan [22] investigated heat transfer effects in the mixed convection flow between concentric vertical cylinders with porous layers.

Bejan [23] investigated minimization of entropy generation in thermal system and explained that this minimization improves the efficiency of a system. Entropy generation in a Newtonian and non-Newtonian fluid flow in circular pipe or annulus was examined by Dagtekin *et al.* [24], Mahmud and Fraser [25], Mansour and Şahin [26], Pakdemirli and Yilbas [27], Tasnim and Mahmud [28], Yilbas *et al.* [29], Yilmaz [30], Yürüsoy *et al.* [31], Haddad *et al.* [32], Al-Zahranah and Yilbas [33]. Influence of slip conditions on forced convection and on entropy generation in a porous saturated circular channel was investigated by Chauhan and Kumar [34].

Several fluids used in engineering and industrial processes, such as poly liquid foams and geological materials, exhibit flow properties that cannot be explained by Newtonian fluid flow model. One of such material models consists of a differential-type fluid, namely, third-grade non-Newtonian fluid which can predict such effects. The objective of this study is to determine the temperature

and velocity distributions in the annular region of a third-grade fluid flow with porous layer, and to obtain the rate of heat transfer and entropy generation number as a function of the pertinent parameters under the assumption of a steady-state laminar fluid flow, fully developed both thermally and hydrodynamically.

2 Formulation of the problem

A non-Newtonian third grade fluid flow through an annular pipe is considered, where a fluid-saturated porous medium layer of very small permeability is perfectly attached to the outer boundary of the annulus as shown in the schematic diagram (Fig. 1). Radius of inner pipe and outer pipe are taken as r_1^* and r_0^* respectively and $(r_0^* - r_2^*)$ is taken as the thickness of the porous layer. In the clear fluid region $(r_1^* < r^* < r_2^*)$ constant pressure gradient is applied in the axial direction. The flow in the porous medium is modeled by Darcy's law hence the flow is assumed to be zero in the porous region $(r_2^* < r^* < r_0^*)$ in the absence of any external pressure gradient and very small permeability of the porous layer. The inner and outer impermeable boundaries of the annulus are maintained at a constant temperature t_w. Viscosity of the fluid is assumed to be temperature-dependent.

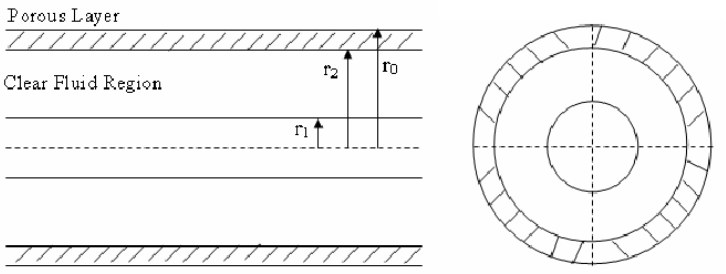

Figure 1: Schematic diagram of the problem

For the present investigation, we seek velocity and temperature fields in the following form:

$$V = w\,(r)\,e_z, \tag{1}$$

$$t_1 = t_1\,(r)\,, \tag{2}$$

$$t_2 = t_2\,(r)\,. \tag{3}$$

The equations which govern the fluid flow are given by

$$divV = 0, \tag{4}$$

$$\rho \frac{DV}{Dt} = divT, \tag{5}$$

where $\mathbf{V}$ is the velocity vector; ρ, the fluid density; T, the Cauchy stress tensor; and, $\frac{D}{Dt} \equiv \frac{\partial}{\partial t} + V.\nabla$, the material time derivative.

The constitutive equation for an incompressible third order fluid is given by (Rivlin and Ericksen [35])

$$T = -pI + \mu A_1 + \alpha_1 A_2 + \alpha_2 A_1^2 + \beta_1 A_3 + \beta_2 \left[A_1 A_2 + A_2 A_1\right] + \beta_3 \left(trA_1^2\right) A_1, \tag{6}$$

where p is the hydrostatic pressure; $\mathbf{I}$, the identity tensor; μ, the coefficient of viscosity and $\alpha_1,\ \alpha_2,\ \beta_1,\ \beta_2\ and\ \beta_3$ are the material constants.

Here, the Rivlin-Ericksen tensors are given by

$$A_1 = L + L^T,$$

$$A_n = \frac{D}{Dt} A_{n-1} + A_{n-1} L + L^T A_{n-1}, \quad (n > 1)$$

and $L = \nabla V$.

Following Fosdick and Rajagopal [36], the material parameters must satisfy

$$\mu \geq 0,\ \alpha_1 \geq 0,\ |\alpha_1 + \alpha_2| \leq \sqrt{24\mu\beta_3},\ \ \beta_1 = \beta_2 = 0,\ \beta_3 \geq 0. \tag{7}$$

We assume, in our analysis that the non-Newtonian fluid is thermodynamically compatible. Thus the Cauchy stress tensor for thermodynamically compatible third grade fluid reduces to

$$T = -pI + \mu A_1 + \alpha_1 A_2 + \alpha_2 A_1^2 + \beta_3 \left(trA_1^2\right) A_1. \tag{8}$$

The energy equation for the present problem is given by

$$\rho \frac{dE}{dt} = \mathbf{T} : \mathbf{L} - div\mathbf{q}, \tag{9}$$

where E is the specific internal energy; and $\mathbf{q}$, is the heat flux vector.

Using Fourier's law, we have

$$divq = -k \left(\frac{1}{r}\frac{d\theta}{dr} + \frac{d^2\theta}{dr^2}\right) \tag{10}$$

for the present geometry, where the constant k is the thermal conductivity.

Using equations (1-10) and following Massoudi and Christie [37], for the fully developed, steady state flow in the clear fluid region ($r_1^* < r^* < r_2^*$) the equations of motion of a third-grade fluid with heat transfer are given by

$$\mu^* \left(\frac{d^2w}{dr^{*2}} + \frac{1}{r^*}\frac{dw}{dr^*} \right) + \frac{d\mu^*}{dr^*}\frac{dw}{dr^*} + \frac{2\beta_3}{r^*}\left(\frac{dw}{dr^*}\right)^2 \left(\frac{dw}{dr^*} + 3r^*\frac{d^2w}{dr^{*2}} \right) = \frac{dp}{dz^*}, \quad (11)$$

$$k\left(\frac{d^2t_1}{dr^{*2}} + \frac{1}{r^*}\frac{dt_1}{dr^*} \right) + \left(\frac{dw}{dr^*}\right)^2 \left[\mu^* + 2\beta_3 \left(\frac{dw}{dr^*}\right)^2 \right] = 0. \quad (12)$$

A Darcy model for the fluid flow in the porous layer attached to the outer boundary of the annulus is used. It is recognized at the outset that for a typical porous medium whose permeability is very small, the fluid flow in the porous medium will be small compared to that outside the porous medium. Thus the main effect of this layer is to introduce slip at the outer boundary of the annulus and to change the value of the thermal conductivity (effective thermal conductivity) in the porous medium. Beavers-Joseph [38] slip boundary condition is used to model the interface between the clear fluid and porous medium.

The flow in the porous layer is assumed to be zero and the energy equation in the fluid-saturated region ($r_2^* < r^* < r_0^*$) is given by

$$\bar{k}\left(\frac{d^2t_2}{dr^{*2}} + \frac{1}{r^*}\frac{dt_2}{dr^*} \right) = 0. \quad (13)$$

The corresponding matching and boundary conditions are given by

$$\begin{aligned} &at \quad r^* = r_1^*; \quad w = 0, \quad t_1 = t_w, \\ &at \quad r^* = r_2^*; \quad \tau_{rz} = \frac{-\alpha}{\sqrt{K_0}}\mu^* w, \quad t_1 = t_2, \quad k\frac{dt_1}{dr^*} = \bar{k}\frac{dt_2}{dr^*}, \\ &at \quad r^* = r_0^*; \quad t_2 = t_w, \end{aligned} \quad (14)$$

where, r^* and z^* are radial and axial coordinates respectively; w, the axial velocity; p, the pressure; μ^*, the viscosity; β_3, the non-Newtonian parameter; t_1, the temperature in the clear fluid region; k, the thermal conductivity of the clear fluid; t_2, the temperature in the porous region; $\bar{k}$, effective thermal conductivity in the porous medium; K_0, the permeability of the porous medium; and α is a constant depending upon the structure of the porous medium.

By introducing the following non-dimensional quantities

$$R_1 = \frac{r_1^*}{r_0^*},\ R_2 = \frac{r_2^*}{r_0^*},\ r_0 = \frac{3r_0^*}{r_0^* - r_1^*},\ r_1 = \frac{3r_1^*}{r_0^* - r_1^*},\ r_2 = \frac{3r_2^*}{r_0^* - r_1^*},\ r = \frac{3r^*}{r_0^* - r_1^*},$$

$$v = \frac{w}{V_0},\ \theta_1 = \frac{t_1 - t_w}{t_m - t_w},\ \theta_2 = \frac{t_2 - t_w}{t_m - t_w},\ \mu = \frac{\mu^*}{\mu_0},\ K = \frac{9K_0}{(r_0^* - r_1^*)^2}, \tag{15}$$

the equations (11-14) reduce to the following:

$$\mu\left(\frac{d^2v}{dr^2} + \frac{1}{r}\frac{dv}{dr}\right) + \frac{d\mu}{dr}\frac{dv}{dr} + \frac{\Lambda}{r}\left(\frac{dv}{dr}\right)^2\left(\frac{dv}{dr} + 3r\frac{d^2v}{dr^2}\right) = C, \tag{16}$$

$$\frac{d^2\theta_1}{dr^2} + \frac{1}{r}\frac{d\theta_1}{dr} + \Gamma\left(\frac{dv}{dr}\right)^2\left[\mu + \Lambda\left(\frac{dv}{dr}\right)^2\right] = 0, \tag{17}$$

$$\frac{d^2\theta_2}{dr^2} + \frac{1}{r}\frac{d\theta_2}{dr} = 0, \tag{18}$$

and the corresponding matching and boundary conditions:

$$\begin{aligned} &at \quad r = r_1; v = 0, \theta_1 = 0, \\ &at \quad r = r_2; \mu\frac{dv}{dr} + \Lambda\left(\frac{dv}{dr}\right)^3 = \frac{-\alpha}{\sqrt{K}}\mu v, \theta_1 = \theta_2, \frac{d\theta_1}{dr} = \varphi\frac{d\theta_2}{dr}, \\ &at \quad r = r_0; \quad \theta_2 = 0, \end{aligned} \tag{19}$$

where, V_0 is the reference velocity; t_m, the mean temperature; $\Gamma = \mu_0 V_0^2/k(t_m - t_w)$, the Brinkman number; $\Lambda = 18\beta_3 V_0^2/\mu_0(r_0^* - r_1^*)^2$, the dimensionless non-Newtonian parameter; $C = \frac{dp}{dz}(r_0^* - r_1^*)^2/9\mu_0 V_0$, the dimensionless pressure gradient; and $\phi = \bar{k}/k$ is the ratio of thermal conductivities.

For the variation of viscosity with temperature, we assume the Reynold's model,

$$\mu = \exp(-M\theta_1) \approx 1 - M\theta_1. \tag{20}$$

Also let $\Lambda = \varepsilon\lambda$ and $M = \varepsilon m$, where, ε is the perturbation parameter; M, the exponential constant for Reynold's model viscosity; m, the ordered viscosity parameter; and λ is the ordered non-Newtonian coefficient.

For obtaining an approximate solution of the problem, we apply perturbation series method.

Let us assume

$$v = v_0 + \varepsilon v_1 + ..., \tag{21}$$

$$\theta_1 = \theta_{10} + \varepsilon\theta_{11} + ..., \tag{22}$$

$$\theta_2 = \theta_{20} + \varepsilon\theta_{21} + ..., \tag{23}$$

and

$$\mu = 1 - \varepsilon m\theta_{10} + ... \tag{24}$$

Substituting (21-24) into equations (16-19), and equating the coefficients of $\varepsilon^0, \varepsilon^1, ...$ on both sides, the following zeroth and first order equations are obtained:

$$\frac{d^2v_0}{dr^2} + \frac{1}{r}\frac{dv_0}{dr} = C, \tag{25}$$

$$\frac{d^2\theta_{10}}{dr^2} + \frac{1}{r}\frac{d\theta_{10}}{dr} + \Gamma\left(\frac{dv_0}{dr}\right)^2 = 0, \tag{26}$$

$$\frac{d^2\theta_{20}}{dr^2} + \frac{1}{r}\frac{d\theta_{20}}{dr} = 0, \tag{27}$$

$$\frac{d^2v_1}{dr^2} + \frac{1}{r}\frac{dv_1}{dr} - m\theta_{10}\left(\frac{d^2v_0}{dr^2} + \frac{1}{r}\frac{dv_0}{dr}\right)$$

]

$$-m\frac{d\theta_{10}}{dr}\frac{dv_0}{dr} + \frac{\lambda}{r}\left(\frac{dv_0}{dr}\right)^2\left[\frac{dv_0}{dr} + 3r\frac{d^2v_0}{dr^2}\right] = 0, \tag{28}$$

$$\frac{d^2\theta_{11}}{dr^2} + \frac{1}{r}\frac{d\theta_{11}}{dr} + \Gamma\left[2\frac{dv_0}{dr}\frac{dv_1}{dr} + \left(\frac{dv_0}{dr}\right)^2\left\{\lambda\left(\frac{dv_0}{dr}\right)^2 - m\theta_{10}\right\}\right] = 0, \tag{29}$$

$$\frac{d^2\theta_{21}}{dr^2} + \frac{1}{r}\frac{d\theta_{21}}{dr} = 0, \tag{30}$$

with the corresponding matching and boundary conditions:

$$\begin{aligned}
&\text{at} \quad r = r_1; \quad v_0 = 0,\ v_1 = 0, \theta_{10} = 0,\ \theta_{11} = 0,\\
&\text{at} \quad r = r_2; \quad \frac{dv_0}{dr} = \frac{-\alpha}{\sqrt{K}}v_0, \frac{dv_1}{dr} + \lambda\left(\frac{dv_0}{dr}\right)^3 = \frac{-\alpha}{\sqrt{K}}v_1,\\
&\qquad\qquad \theta_{10} = \theta_{20},\ \theta_{11} = \theta_{21},\ \frac{d\theta_{10}}{dr} = \varphi\frac{d\theta_{20}}{dr},\ \frac{d\theta_{11}}{dr} = \varphi\frac{d\theta_{21}}{dr},\\
&\text{at} \quad r = r_0; \quad \theta_{20} = 0, \quad \theta_{21} = 0.
\end{aligned} \tag{31}$$

The solutions of (25) to (30) subject to the boundary/matching conditions (31) are determined, and the approximate solutions for velocity and temperature

profiles are obtained as follows:

$$v = \frac{Cr^2}{4} + a_1 \log r + a_2 + \varepsilon \left\{ \frac{b_0}{r^2} + b_1 r^2 - b_2 r^4 - b_3 r^6 + b_4 r^2 \log r \right. \tag{32}$$
$$\left. + b_5 (\log r)^2 - b_6 (r \log r)^2 - b_7 (\log r)^3 + a_7 \log r + a_8 \right\},$$
$$\theta_1 = -\Gamma \left\{ \frac{C^2 r^4}{64} + \frac{C a_1 r^2}{4} + \frac{a_1^2}{2} (\log r)^2 \right\} + a_3 \log r + a_4$$
$$+ \varepsilon \left[c_1 r^8 + c_2 r^6 + r^4 \left\{ c_3 (\log r)^2 + c_4 \log r + c_5 \right\} \right. \tag{33}$$
$$+ r^2 \left\{ c_6 (\log r)^2 + c_7 \log r + c_8 \right\} + c_9 (\log r)^4$$
$$\left. + \ c_{10} (\log r)^3 + c_{11} (\log r)^2 + \frac{c_{12}}{r^2} + a_9 \log r + a_{10} \right],$$
$$\theta_2 = a_5 \log r + a_6 + \varepsilon \{ a_{11} \log r + a_{12} \}, \tag{34}$$

where, the constants of integration $a_1, a_2, ..., a_{12}$ are reported in the appendix.

2.1 Entropy generation

Following Bejan [23] the dimensionless entropy generation number in the clear fluid region is given by

$$Ns = \left\{ \frac{1}{(\theta_1 + \theta_0)^2} \left(\frac{d\theta_1}{dr} \right)^2 \right\} + \left\{ \Gamma \frac{1}{(\theta_1 + \theta_0)} \left(\frac{dv}{dr} \right)^2 \left[\mu + \Lambda \left(\frac{dv}{dr} \right)^2 \right] \right\}, \tag{35}$$

$$= Ns_1 + Ns_2, \tag{36}$$

where $Ns = \frac{S'''_{gen}}{S'''_G}$; $S'''_G = \frac{9k}{(r_0^* - r_1^*)^2}$; $\theta_0 = \frac{t_w}{(t_m - t_w)}$; Ns_1, is the term due to heat generation; and Ns_2, is the term due to viscous dissipation.

Since the flow in the porous region is assumed to be zero, entropy generation in this region is only due to heat transfer, and it is given by

$$Ns' = \frac{\varphi}{(\theta_2 + \theta_0)^2} \left(\frac{d\theta_2}{dr} \right)^2. \tag{37}$$

3 Discussion

Non-Newtonian third-grade fluid flow is considered in an annulus with a porous layer of very small permeability attached to the outer boundary, and the heat

transfer effects are investigated on this flow in annulus by taking temperature-dependent viscosity of the fluid. Entropy analysis of the annular flow is also carried out because the thermodynamic irreversibility can be quantified through entropy generation, and its minimization improves system efficiency as explained by Bejan [23] and many other researchers.

Fig.2 shows the variations of velocity profiles along the radial distance in the annulus for different values of the non-Newtonian parameter (Λ) and the viscosity coefficient parameter (M). It is seen that the magnitude of the maximum velocity in the annulus increases by reducing the non-Newtonian parameter. Velocity profiles are also compared with that of Newtonian fluid ($\Lambda = 0$) case. Velocity is enhanced in the annulus with the increase in the value of the viscosity coefficient parameter (M). Because the parameter M increases by reducing the viscosity, hence the rate of fluid strain enhances near boundaries and maximum velocity increases in the annulus. Fig. 3 shows the velocity profiles along the radial distance in the annulus for different values of the permeability parameter (K) and the Brinkman number (Γ). It is seen that there is a slip at the outer porous interface, which increases by increasing the permeability parameter. Consequently the flow in the annulus enhances with the increase in K value, and the maximum velocity moves towards the outer porous boundary in the annulus. As Brinkman number increases the maximum velocity in the annulus also increases.

Fig.4 and 5 show the variation of temperature field in the annulus for different values of the non-Newtonian parameter (Λ), viscosity coefficient parameter (M), Brinkman number (Γ), thermal conductivity ratio (φ) and the permeability parameter (K). It is found that the temperature in the annulus increases with reducing the value of non-Newtonian parameter. It is seen that the temperature gradient decays gradually due to the diffusion of heat transfer in the middle part of the annulus. The effect of the Brinkman number or viscosity coefficient parameter is to increase temperature in both clear fluid and porous region of the annulus. However, conductivity ratio (φ) reduces it in the annulus. Further it is seen that the maximum value of the temperature shifts to the inner side in the annulus as φ increases. The permeability (K) of the porous layer significantly influences temperature distribution in the annulus. It is noticed that by increasing the value of K, temperature in the porous region and near it decreases while temperature increases in the region near the inner cylinder.

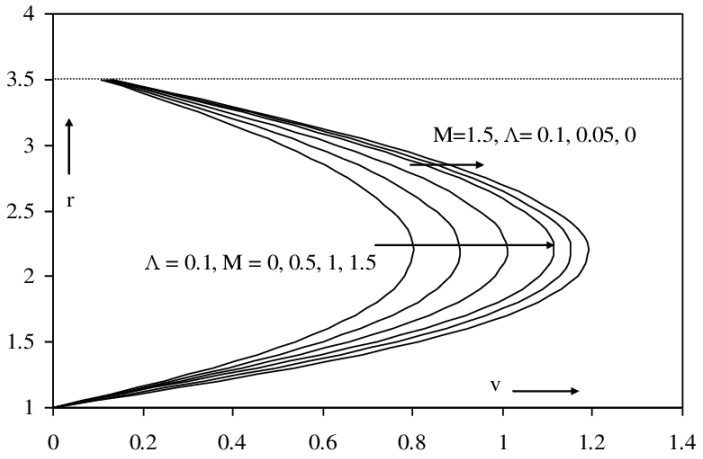

Figure 2: Velocity profiles vs r for $C = -1,\ \Gamma = 1,\ \alpha = 0.1,\ K = 0.0001,\ \varepsilon = 0.1,\ \varphi = 1.5$.

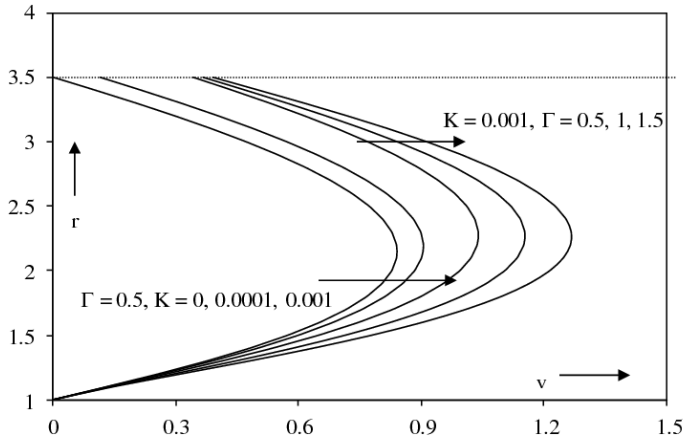

Figure 3: Velocity profiles vs r for $C = -1,\ \Lambda = 0.1,\ \alpha = 0.1,\ M = 1,\ \varepsilon = 0.1,\ \varphi = 1.5$

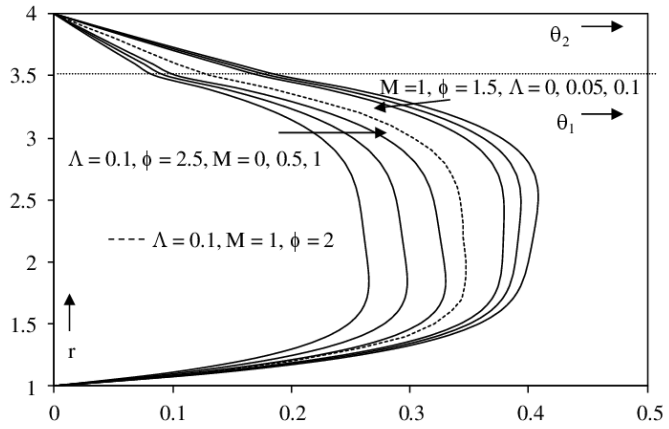

Figure 4: Temperature profiles vs r for $C = -1$, $\Gamma = 1$, $\alpha = 0.1$, $K = 0.0001$, $\varepsilon = 0.1$

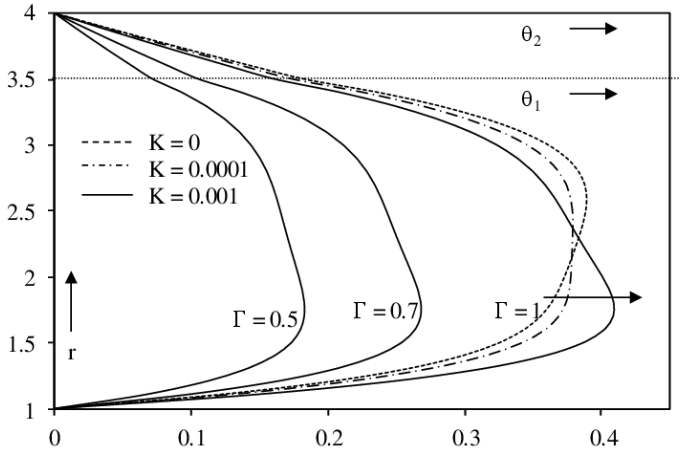

Figure 5: Temperature profiles vs r for $C = -1$, $\Lambda = 0.1$, $\alpha = 0.1$, $M = 1$, $\varepsilon = 0.1$, $\varphi = 1.5$

Table 1: Temperature gradient at $r = 1$ for $C = -1, \alpha = 0.1,\ \varepsilon = 0.1$.

Γ	Λ	M	ϕ	K	$(d\theta_1/dr)_{r=1}$
1	0.1	1	1.5	0.0001	1.409573
0.5	0.1	1	1.5	0.0001	0.634602
0.3	0.1	1	1.5	0.0001	0.363917
0.1	0.1	1	1.5	0.0001	0.115691
1	0.05	1	1.5	0.0001	1.474032
1	0	1	1.5	0.0001	1.538491
1	0.1	0.5	1.5	0.0001	1.269204
1	0.1	0	1.5	0.0001	1.128834
1	0.1	1	2	0.0001	1.343574
1	0.1	1	2.5	0.0001	1.303563
1	0.1	1	1.5	0.00001	1.351478
1	0.1	1	1.5	0	1.325552

The variation of rate of heat transfer is reported in Table 1 for different values of the pertinent parameters. It is found that increasing the thermal conductivity ratio (φ) leads to a reduction in the rate of heat transfer at the inner cylindrical boundary of the annulus. It also decreases with increasing non-Newtonian parameter (Λ) value, while the permeability (K) of the porous layer enhances the rate of heat transfer at the inner boundary of the annulus. The same effect is observed with the viscosity coefficient parameter (M) and the Brinkman number (Γ).

Entropy generation number (Ns_1)due to heat transfer in the annulus for different values of the pertinent parameters is plotted against radial distance in Fig.6 (a & b). It is seen that the entropy generation number (Ns_1) is very low in the middle part of the annulus because of gradually varying small temperature gradient there, and attains high values in the vicinity of the inner cylindrical boundary, porous interface and in the porous layer attached to the outer boundary of the annulus. It is more pronounced in the region near the inner boundary of the annulus because of high temperature gradient there. Further it decays sharply near the annular boundaries because the high rate of heat transfer takes

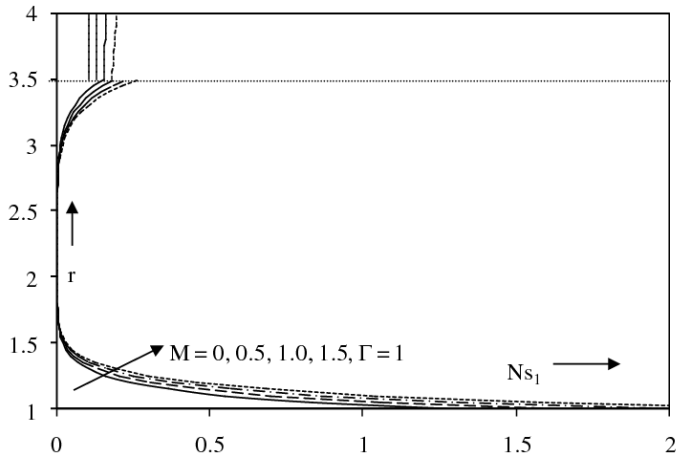

(a)

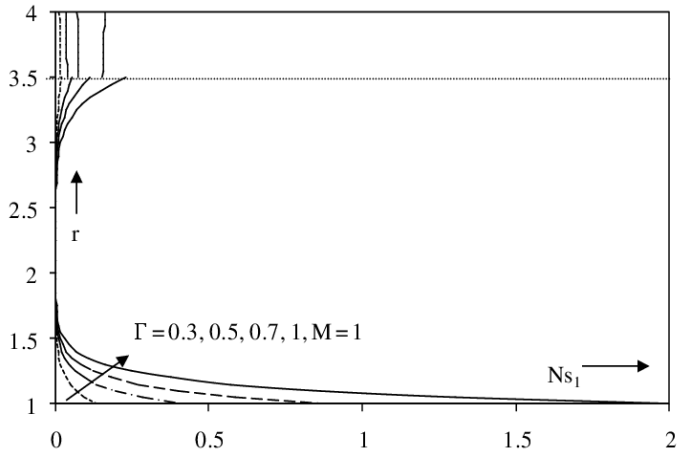

(b)

Figure 6: Ns_1 vs r for $C = -1,\ \Lambda = 0.1,\ K = 0.0001,\ \varphi = 1.5,\ \theta_0 = 1,\ \alpha = 0.1,\ \varepsilon = 0.1$.

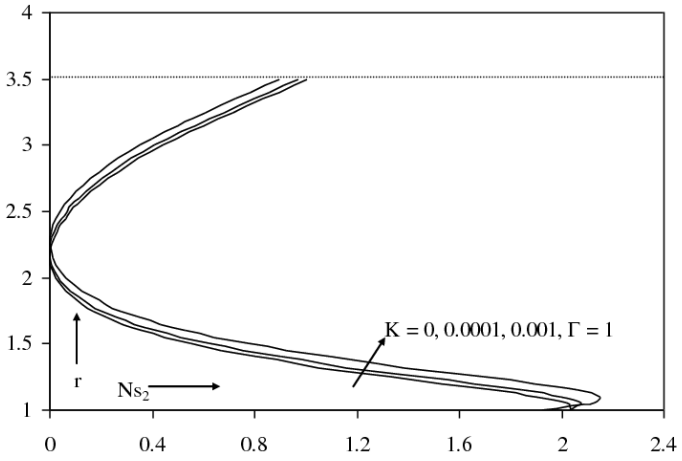

(a)

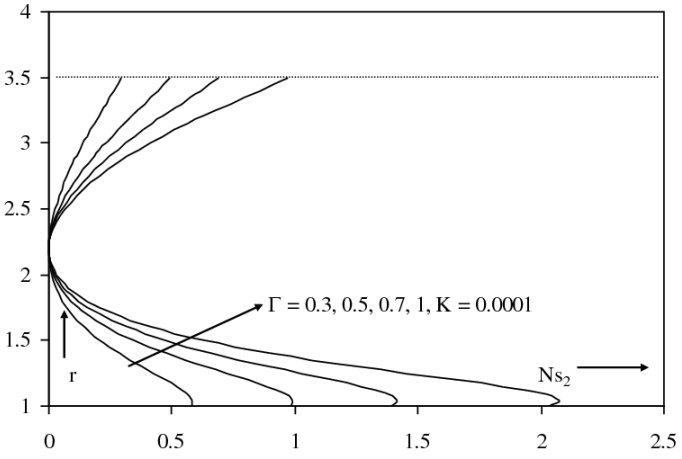

(b)

Figure 7: Ns_2 vs r for $C = -1,\ M = 1,\ \Lambda = 0.1,\ \varphi = 1.5,\ \theta_0 = 1,\ \alpha = 0.1,\ \varepsilon = 0.1$.

place in this part of the annulus. It is seen that the viscosity coefficient parameter (M) as well as the Brinkman number (Γ) enhances the entropy generation number (Ns_1) in the annulus and also in the porous layer.

Fig.7 (a & b) shows entropy generation number (Ns_2) due to fluid friction for different values of the permeability parameter (K) and the Brinkman number (Γ). It attains high values near the annulus boundaries because of high fluid strain there. It is seen that Ns_2 decreases close to the inner boundary by increasing the permeability (K) of the porous layer, then increases sharply in the nearby region. However it decreases near the porous interface in the annulus by K. The effect of Brinkman number (Γ) is to increase Ns_2, and it attains high values particularly in the region near to the inner boundary of the annulus.

Figs.8-11 depict the total entropy generation number (Ns) at different locations ($r = 1,\ r = 2,\ r = 3.5$) in the annulus. It is seen that increasing the value of the non-Newtonian parameter (Λ) lowers sharply the total entropy generation number (Ns) particularly close to the inner boundary region; however the effect is insignificant at the outer porous interface ($r = 3.5$) and for the central region ($r = 2$). The viscosity coefficient parameter (M) increases the total entropy generation number at both radial locations ($r = 1,\ r = 3.5$) and the effect is insignificant at the location corresponding to $r = 2$. The effect of the permeability is insignificant on the entropy generation number (Ns) at the locations $r = 2$ and$r = 3.5$, however, Ns enhances slightly as K increases at $r = 1$. Brinkman number (Γ) enhances significantly the entropy generation number at all locations except in the region corresponding to $r = 2$.

Conclusions

The conclusions of the present study are as follows:

1. Effect of the non-Newtonian parameter (Λ) is to decrease the flow in the annulus, while viscosity coefficient parameter(M), or permeability parameter(K), or Brinkman number (Γ) enhances flow.

2. Effect of parameter Λ is to decrease temperature while parameter Γ or M enhances it. Increasing value of K, temperature in the porous and nearly region decreases and near inner boundary it increases.

3. Effect of the parameters Λ or φ, is to reduce rate of heat transfer at the inner boundary of the annulus while parameter K, or M, or Γ enhances it.

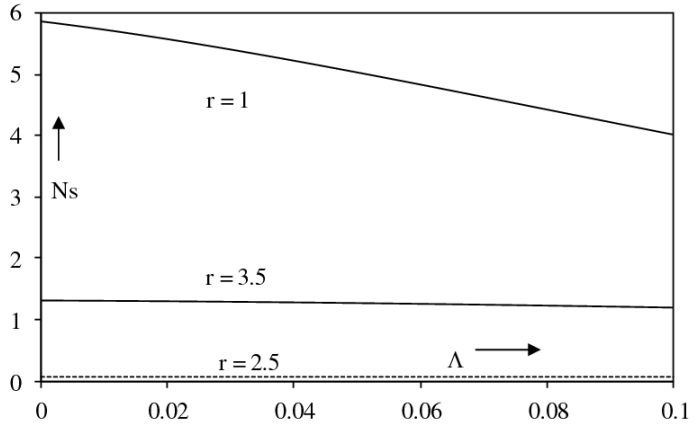

Figure 8: *Ns* vs Λfor $C = -1,\ \Gamma = 1,\ M = 1,\ K = 0.0001,\ \varphi = 1.5,\ \theta_0 = 1,\ \alpha = 0.1,\ \varepsilon = 0.1.$

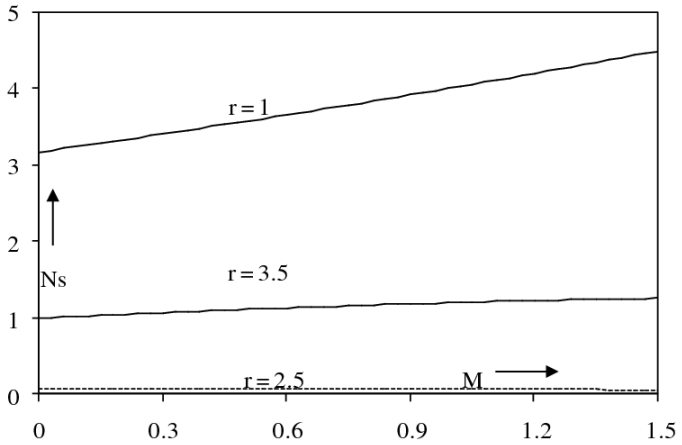

Figure 9: *Ns* vs M for $C = -1,\ \Gamma = 1,\ \Lambda = 0.1,\ K = 0.0001,\ \varphi = 1.5,\ \theta_0 = 1,\ \alpha = 0.1,\ \varepsilon = 0.1.$

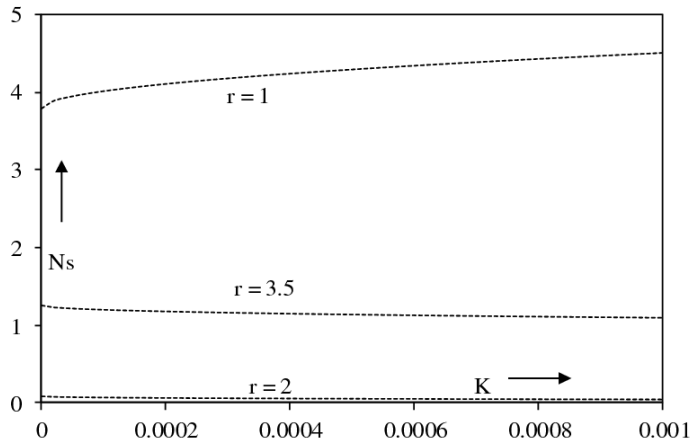

Figure 10: *Ns* vs K for $C = -1,\ \Gamma = 1,\ M = 1,\ \Lambda = 0.1,\ \varphi = 1.5,\ \theta_0 = 1,\ \alpha = 0.1,\ \varepsilon = 0.1$.

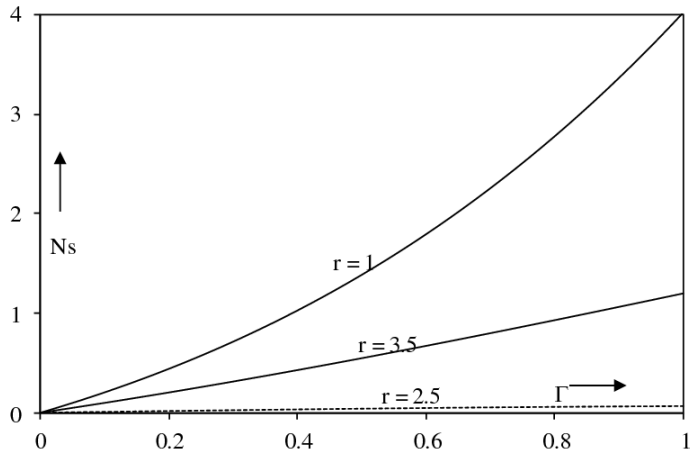

Figure 11: *Ns* vs Γ for $C = -1,\ \Lambda = 0.1,\ M = 1,\ K = 0.0001,\ \varphi = 1.5,\ \theta_0 = 1,\ \alpha = 0.1,\ \varepsilon = 0.1$.

4. The parameter M or Γ increases the entropy generation number due to heat transfer (Ns_1) in the annulus. Effect of the parameter Γ is to increase the entropy generation number due to fluid friction (Ns_2), while the parameter K reduces it near the porous interface. Further, effect of parameter Λ is to decrease the total entropy generation number (Ns) while M or Γ enhances it. However, the effect of the permeability parameter is insignificant.

Acknowledgement

We express our thanks to the referees for their fruitful advices and comments. The support provided by CSIR (Council of Scientific and Industrial Research) through Senior Research Fellowship to one of the authors Vikas Kumar is gratefully acknowledged.

References

[1] A.S.Berman, *Laminar flow in an annulus with porous walls*, J. Appl. Phys., 29 (1958), 71-75.

[2] J.N. Kapur and S.Goel, *Flow of a non-Newtonian fluid between rotating cylinders with suction and injection*, Phys. Fluids, 6(1963), 626-631.

[3] S.P.Mishra and J.S.Roy, *Laminar elasticoviscous flow in an annulus with porous walls*, Phys. Fluids, 10(1967), 2300-2304.

[4] S.P.Mishra and J.S.Roy, *Flow of elasticoviscous liquid between rotating cylinders with suction and injection*, Phys. Fluids, 11(1968), 2074-2081.

[5] A.M.Hecht, *Theoretical non-Newtonian pipe-flow heat transfer*, AIChE J., 19(1973), 197-199.

[6] H.G.Sharma and K.R.Singh, *Heat transfer in the laminar flow of a non-Newtonian fluid in a porous annulus by the method of quasi linearization*, Int. J. Heat Mass Transfer, 30(1987), 1227-1231.

[7] R.Bhatnagar, H.W.Vayo and D.Okunbor, *Application of quasilinearization to viscoelastic flow through porous annulus*, Int. J. Non-Linear Mech., 29(1994), 13-22.

[8] Y.Wang and G.A.Chukwu, *Unsteady axial laminar Couette flow of power-law fluids in a concentric annulus*, Industrial and Engineering Chemistry Research, 35(1996), 2039-2047.

[9] M.Yürüsoy and M.Pakdemirli, *Approximate analytical solutions for the flow of a third-grade fluid in a pipe*, Int. J. Non linear Mech., 37(2002), 187–195.

[10] M.Yürüsoy, *Flow of a third grade fluid between concentric circular cylinders*, Math. Comput. Appl., 9(2004), 11–17.

[11] M.E.Erdogan and C.E.İmrak, *Steady flow of a second-grade fluid in an annulus with porous walls*, Mathematical Problems in Engineering, 2008(2008), 1-11. (doi:10.1155/2008/867906)

[12] S.Chikh, A.Boumedien, K.Bouhadef and G.Lauriat, *Analytical solution of non-Darcian forced convection in an annular duct partially filled with a porous medium*, Int. J. Heat Mass Transfer, 38(1995), 1543-1551.

[13] Y.Demirel and R.Kahraman, *Thermodynamic analysis of convective heat transfer in an annular packed bed*, Int. J. Heat Fluid Flow, 21(2000), 442–448.

[14] N.D.Scurtu, A.Postelnicu and I.Pop, *Free convection between two horizontal concentric cylinders filled with a porous medium- a perturbed solution*, Acta Mechanica, 151(2001), 115-125.

[15] A.Haji-Sheikh, *Estimation of average and local heat transfer in parallel plates and circular ducts filled with porous materials*, ASME J. Heat Transfer, 126(2004), 400-409.

[16] W.J.Minkowycz and A.Haji-Sheikh, *Heat transfer in parallel plates and circular porous passages with axial conduction*, Int. J. Heat Mass Transfer, 49(2006), 2381-2390.

[17] K.Hooman and H.Gurgenci, *A theoretical analysis of forced convection in a porous-saturated circular tube: Brinkman-Forchheimer model*, Trans. Porous Media, 69(2007), 289-300.

[18] K.Hooman, A.Pourshaghaghy and A.Ejlali, *Effects of viscous dissipation on thermally developing forced convection in a porous saturated circular tube with an isoflux wall*, Appl. Math. Mech.-Engl. Ed., 27(2006), 617-626.

[19] K.Hooman, A.A.Ranjbar-Kani and A.Ejlali, *Axial conduction effects on thermally developing forced convection in a porous medium: circular tube with uniform wall temperature*, Heat Transfer Research, 34(2003), 34-40.

[20] A.V.Kuznetsov, D.A.Nield and M.Xiong, *Thermally developing forced convection in a porous medium: circular duct with walls at constant temperature, with longitudinal conduction and viscous dissipation effects*, Transport Porous Media, 53(2003), 331-345.

[21] K.Khanafer, A.Al-Amiri and I.Pop, *Numerical analysis of natural convection heat transfer in a horizontal annulus partially filled with a fluid-saturated porous substrate*, Int. J. of Heat and Mass Transfer, 51(2008), 1613-1627.

[22] M.S.Al-Zahrani and S.Kiwan, *Mixed convection heat transfer in the annulus between two concentric vertical cylinders using porous layers*, Transp. Porous Med., 76(2009), 391–405.

[23] A.Bejan, Entropy generation minimization, CRC Press, Florida, 1996.

[24] Ī.Dağtekin, H.F.Öztop and A.Z.Şahin, *An analysis of entropy generation through a circular duct with different shaped longitudinal fins for laminar flow*, Int. J. Heat Mass Transfer, 48(2005), 171-181.

[25] S.Mahmud and R.A.Fraser, *Irreversibility analysis of concentrically rotating annuli*, Int. Comm. Heat Mass Transfer, 29(2002), 697–706.

[26] R.B.Mansour and A.Z. Şahin, *Entropy generation in developing laminar fluid flow through a circular pipe with variable properties*, Heat Mass Transfer, 42(2005), 1–11.

[27] M.Pakdemirli and B.S.Yilbas, *Entropy generation in a pipe due to non-Newtonian fluid flow: constant viscosity case*, Sadhana, 31(2006), 21–29.

[28] S.H.Tasnim and S.Mahmud, *Entropy generation in a vertical concentric channel with temperature dependent viscosity*, Int. Comm. Heat Mass Transfer, 29(2002), 907–918.

[29] B.S.Yilbas, M.Yürüsoy and M.Pakdemirli, *Entropy analysis for non-Newtonian fluid flow in annular pipe: constant viscosity case*, Entropy, 6(2004), 304-315.

[30] A.Yilmaz, *Minimum entropy generation for laminar flow at constant wall temperature in a circular duct for optimum design*, Heat Mass Transfer, 45(2009), 1415–1421.

[31] M.Yürüsoy, B.S.Yilbas and M.Pakdemirli, *Non-Newtonian fluid flow in annular pipes and entropy generation: temperature-dependent viscosity*, Sadhana, 31(2006), 683–695.

[32] O.M.Haddad, M.K.Alkam and M.T.Khasawneh, *Entropy generation due to laminar forced convection in the entrance region of a concentric annulus*, Energy, 29(2004), 35–55.

[33] I.T.Al-Zaharnah and B.S.Yilbas, *Thermal analysis in pipe flow: influence of variable viscosity on entropy generation*, Entropy, 6(2004), 344–363.

[34] D.S.Chauhan andV.Kumar, *Effects of slip conditions on forced convection and entropy generation in a circular channel occupied by a highly porous medium: Darcy extended Brinkman-Forchheimer model*, Turk. J. Eng. Env. Sci., 33(2009), 91-104.

[35] R.S.Rivlin and J.L.Ericksen, *Stress deformation relation for isotropic materials*, J. Rat. Mech. Anal., 4(1955), 323-425.

[36] R.L.Fosdick and K.R.Rajagopal, *Thermodynamics and stability of fluids of third grade*, Proc. Royal Soc. Lon. A, 339(1980), 351-377.

[37] M.Massoudi and I.Christie, *Effects of variable viscosity and viscous dissipation on the flow of a third grade fluid in a pipe*, Int. J. Non linear Mech., 30(1995), 687–699.

[38] G.S.Beavers and D.D.Joseph, *Boundary conditions at a naturally permeable wall*, J. Fluid Mech., 30(1967), 197-207.

Appendix

$$a_1 = \frac{-Cr_2\left[2r_2\sqrt{K}+\alpha\left(r_2^2-r_1^2\right)\right]}{4\left[\sqrt{K}+\alpha r_2\left(\log r_2-\log r_1\right)\right]}, \qquad a_2 = \frac{-Cr_1^2}{4} - a_1\log r_1,$$

$$a_3 = \varphi a_5 + \Gamma\left(\frac{C^2r_2^4}{16}+\frac{Ca_1r_2^2}{2}+a_1^2\log r_2\right), \quad a_6 = -a_5\log r_0,$$

$$a_4 = -a_3\log r_1 + \Gamma\left\{\frac{C^2r_1^4}{16}+\frac{Ca_1r_1^2}{2}+\frac{a_1^2}{2}\left(\log r_1\right)^2\right\},$$

$$a_5 = \Gamma\left[\log\left(r_2/r_1\right)\left\{\frac{C^2r_2^4}{16}+\frac{Ca_1r_2^2}{2}+a_1^2\log r_2\right\} - \left\{\frac{C^2}{64}\left(r_2^4-r_1^4\right)\right.\right.$$
$$\left.\left. + \frac{Ca_1}{4}\left(r_2^2-r_1^2\right)+\frac{a_1^2}{2}\left(\left(\log r_2\right)^2-\left(\log r_1\right)^2\right)\right\}\right]\left\{log(r_2/r_0)-\varphi log(r_2/r_1)\right\}^{-1},$$

$$a_7 = \Big[2b_0/r_2^3 - 2b_1r_2 + 4b_2r_2^3 + 6b_3r_2^5 - 2b_4r_2\log r_2 - b_4r_2 - \left(2b_5/r^2\right)\log r_2 + 2b_6r_2\left(\log r_2\right)^2$$
$$+2b_6r_2\log r_2 + 3(b_7/r_2)\left(\log r_2\right)^2 - \lambda\left(Cr_2/2+a_1/r_2\right)^3 - \frac{\alpha}{\sqrt{K}}\left\{b_0\left(1/r_2^2-1/r_1^2\right)\right.$$
$$+b_1\left(r_2^2-r_1^2\right) - b_2\left(r_2^4-r_1^4\right) - b_3\left(r_2^6-r_1^6\right) + b_4\left(r_2^2\log r_2 - r_1^2\log r_1\right) + b_5\left(\left(\log r_2\right)^2\right.$$
$$\left. - \left(\log r_1\right)^2\right) - b_6\left(r_2^2(\log r_2)^2 - r_1^2(\log r_1)^2\right) - b_7\left(\left(\log r_2\right)^3-\left(\log r_1\right)^3\right)\Big] / \{1/r_2$$
$$\left. + \frac{\alpha}{\sqrt{K}}\log\left(r_2/r_1\right)\right\},$$

$$a_8 = -a_7\log r_1 - \Big\{b_0/r_1^2 + b_1r_1^2 - b_2r_1^4 - b_3r_1^6 + b_4r_1^2\log r_1 + b_5\left(\log r_1\right)^2,$$
$$- b_6r_1^2\left(\log r_1\right)^2 - b_7\left(\log r_1\right)^2\Big\},$$

$$a_9 = \varphi a_{11} - \left[8c_1r_2^8 + 6c_2r_2^6 + 4r_2^4\left\{c_3(\log r_2)^2 + c_4\log r_2 + c_5\right\}\right.$$
$$+2r_2^2\left\{c_6(\log r_2)^2 + c_7\log r_2 + c_8\right\} + r_2^4(2c_3\log r_2 + c_4)$$
$$\left. + r_2^2(2c_6\log r_2 + c_7) + 4c_9(\log r_2)^3 + 3c_{10}(\log r_2)^2 + 2c_{11}\log r_2 - 2c_{12}/r_2^2\right],$$

$$a_{10} = -\left[a_9\log r_1 + c_1r_1^8 + c_2r_1^6 + r_1^4\left\{c_3(\log r_1)^2 + c_4\log r_1 + c_5\right\} + r_1^2\left\{c_6(\log r_1)^2\right.\right.$$
$$\left.\left. + c_7\log r_1 + c_8\right\} + c_9(\log r_1)^4 + c_{10}(\log r_1)^3 + c_{11}(\log r_1)^2 + c_{12}/r_1^2\right],\Big]$$

$$
\begin{aligned}
a_{11} &= \Big[c_1\left(r_2^8-r_1^8\right)+c_2\left(r_2^6-r_1^6\right)+c_3\left\{r_2^4\left(\log r_2\right)^2-r_1^4\left(\log r_1\right)^2\right\}+c_4\left(r_2^4\log r_2-r_1^4\log r_1\right)\\
&+c_5\left(r_2^4-r_1^4\right)+c_6\left\{r_2^2\left(\log r_2\right)^2-r_1^2\left(\log r_1\right)^2\right\}+c_7\left\{r_2^2\log r_2-r_1^2\log r_1\right\}+c_8\left(r_2^2-r_1^2\right)\\
&+c_9\left\{\left(\log r_2\right)^4-\left(\log r_1\right)^4\right\}+c_{10}\left\{\left(\log r_2\right)^3-\left(\log r_1\right)^3\right\}+c_{11}\left\{\left(\log r_2\right)^2-\left(\log r_1\right)^2\right\}\\
&+c_{12}\left(1/r_2^2-1/r_1^2\right)-\log\left(r_2/r_1\right)\Big[8c_1r_2^8+6c_2r_2^6+4r_2^4\left\{c_3\left(\log r_2\right)^2+c_4\log r_2+c_5\right\}\\
&+r_2^4\left(2c_3\log r_2+c_4\right)+2r_2^2\left\{c_6\left(\log r_2\right)^2+c_7\log r_2+c_8\right\}+r_2^2\left(2c_6\log r_2+c_7\right)+4c_9\left(\log r_2\right)^3\\
&+\ 3c_{10}\left(\log r_2\right)^2+2c_{11}\log r_2-2c_{12}/r_2^2\Big]\Big]\Big/[\log\left(r_2/r_0\right)-\varphi\log\left(r_2/r_1\right)],\\
a_{12} &= -a_{11}\log r_0,\\
b_0 &= \frac{\lambda a_1^3}{2},\quad b_1=\frac{C}{16}\left\{4ma_4-2ma_3-3\Gamma ma_1^2-6Ca_1\lambda\right\},\\
b_2 &= \frac{C^2}{256}\left\{8C\lambda+9\Gamma ma_1\right\},\quad b_3=\frac{C^3\Gamma m}{768},\quad b_4=\frac{Cm}{8}\left(2a_3+\Gamma a_1^2\right),\\
b_5 &= \frac{ma_1a_3}{2},\quad b_6=\frac{\Gamma mCa_1^2}{8},\quad b_7=\frac{\Gamma ma_1^3}{6},\\
&-b_2\left(r_2^4-r_1^4\right)-b_3\left(r_2^6-r_1^6\right)+b_4\left(r_2^2\log r_2-r_1^2\log r_1\right)\\
&+b_5\left(\log r_2\right)^2-\left(\log r_1\right)^2-b_6\left(r_2^2\left(\log r_2\right)^2-r_1^2\left(\log r_1\right)^2\right)\\
&-b_7\left(\left(\log r_2\right)^3-\left(\log r_1\right)^3\right)\Big]/\{1/r_2+\alpha/\sqrt{K}\log(r_2/r_1)\},\\
&-b_6r_1^2\left(\log r_1\right)^2-b_7\left(\log r_1\right)^2\Big\},\\
c_1 &= \frac{3\Gamma Cb_3}{32}-\frac{m\Gamma^2C^4}{16384},\\
c_2 &= \frac{\Gamma b_3}{9}(C+3a_1)-\frac{\lambda\Gamma C^4}{576}-\frac{5m\Gamma^2C^3a_1}{2304},\qquad c_3=\frac{\Gamma Cb_6}{8}-\frac{m\Gamma^2C^2a_1^2}{128},\\
c_4 &= \frac{m\Gamma^2C^2a_1^2}{128}+\frac{m\Gamma a_3C^2}{64}-\frac{\Gamma Cb_4}{8},\\
c_5 &= \frac{m\Gamma C^2}{128}(2a_4-a_3)-\frac{\Gamma C}{64}(b_6+8b_1+2\lambda_1C^2)-\frac{5ma_1^2\Gamma^2C^2}{256}+\frac{\Gamma a_1b_2}{2},
\end{aligned}
$$

$$c_6 = \Gamma a_1 b_6 + \frac{3\Gamma C b_7}{6} - \frac{m a_1^3 \Gamma^2 C}{8},$$

$$c_7 = \frac{m\Gamma C a_1}{4}(\Gamma a_1^2 + a_3) - \frac{\Gamma C}{2}(b_5 + 3b_7) - \Gamma a_1(b_4 + b_6),$$

$$c_8 = \frac{\Gamma C}{8}(9b_7 - 2a_7 + 4b_5) + \frac{\Gamma a_1}{2}(b_6 + b_4 - 2b_1) + \frac{m a_1 \Gamma C}{4}(a_4 - a_3 - \Gamma a_1^2) - \frac{3}{8}\lambda\Gamma C^2 a_1^2,$$

$$c_9 = \frac{\Gamma a_1 b_7}{2} - \frac{m\Gamma^2 a_1^4}{24}, \qquad c_{10} = \frac{m\Gamma a_1^2 a_3}{6} - \frac{2\Gamma a_1 b_5}{3},$$

$$c_{11} = \frac{m\Gamma a_1^2 a_4}{2} - \Gamma a_1 a_7 + \Gamma C(b_0 - \lambda a_1^3), \qquad c_{12} = \Gamma a_1 b_0 - \frac{\lambda\Gamma a_1^4}{4}.$$

Submitted in July 2012, revised in August 2013.

Entropijska analiza za fluid trećeg reda sa viskozitetom zavisnim od temperature u anulusu delimično ispunjenom poroznom sredinom

Posmatra se tečenje nenjutnovske tečnosti trećeg reda sa viskozitetom zavisnim od temperature u anulusu delimično ispunjenom poroznom sredinom veoma malog permeabiliteta. Dobijeno je analitičko rešenje metodom perturbacionim redom za polja brzine i temperature predpostavljajući Rejnoldsov model za varijaciju viskoznosti fluida sa temperaturom. Efekti različitih relevantnih parametara na tečenje fluida, polje temperature i broj generacije entropije su dobijeni i grafiķi diskutovani.

doi:10.2298/TAM1303441C Math. Subj. Class.: 76A05; 76R50; 76S05.